

## Mineralogy and chemistry of cobbles at Meridiani Planum, Mars, investigated by the Mars Exploration Rover Opportunity

I. Fleischer,<sup>1</sup> J. Brückner,<sup>2</sup> C. Schröder,<sup>3,4</sup> W. Farrand,<sup>5</sup> E. Tréguier,<sup>6</sup> R.V. Morris,<sup>7</sup> G. Klingelhöfer,<sup>1</sup> K. Herkenhoff,<sup>8</sup> D. Mittlefehldt,<sup>7</sup> J. Ashley,<sup>9</sup> M. Golombek,<sup>10</sup> J. R. Johnson,<sup>8</sup> B. Jolliff,<sup>11</sup> S. W. Squyres,<sup>12</sup> C. Weitz,<sup>13</sup> R. Gellert,<sup>14</sup> P. A. de Souza,<sup>15</sup> and B. A. Cohen<sup>16</sup>

Received 12 April 2010; revised 12 July 2010; accepted 28 July 2010; published 21 October 2010.

[1] Numerous loose rocks with dimensions of a few centimeters to tens of centimeters and with no obvious physical relationship to outcrop rocks have been observed along the traverse of the Mars Exploration Rover Opportunity. To date, about a dozen of these rocks have been analyzed with Opportunity's contact instruments, providing information about elemental chemistry (Alpha Particle X-ray Spectrometer), iron mineralogy and oxidation states (Mössbauer Spectrometer) and texture (Microscopic Imager). These "cobbles" appear to be impact related, and three distinct groups can be identified on the basis of chemistry and mineralogy. The first group comprises bright fragments of the sulfate-rich bedrock that are compositionally and texturally indistinguishable from outcrop rocks. All other cobbles are dark and are divided into two groups, referred to as the "Barberton group" and the "Arkansas group," after the first specimen of each that was encountered by Opportunity. Barberton group cobbles are interpreted as meteorites with an overall chemistry and mineralogy consistent with a mesosiderite silicate clast composition. Arkansas group cobbles appear to be related to Meridiani outcrop and contain an additional basaltic component. They have brecciated textures, pointing to an impact-related origin during which local bedrock and basaltic material were mixed.

**Citation:** Fleischer, I., et al. (2010), Mineralogy and chemistry of cobbles at Meridiani Planum, Mars, investigated by the Mars Exploration Rover Opportunity, *J. Geophys. Res.*, 115, E00F05, doi:10.1029/2010JE003621.

<sup>1</sup>Institut für Anorganische Chemie und Analytische Chemie, Johannes Gutenberg-Universität, Mainz, Germany.

<sup>2</sup>Max-Planck-Institut für Chemie, Mainz, Germany.

<sup>3</sup>Department of Hydrology, University of Bayreuth, Bayreuth, Germany.

<sup>4</sup>Center for Applied Geoscience, Eberhard Karls University of Tübingen, Tübingen, Germany.

<sup>5</sup>Space Science Institute, Boulder, Colorado, USA.

<sup>6</sup>European Space Astronomy Centre, Villanueva de la Cañada, Spain.

<sup>7</sup>NASA Johnson Space Center, Houston, Texas, USA.

<sup>8</sup>Astrogeology Science Center, U.S. Geological Survey, Flagstaff, Arizona, USA.

<sup>9</sup>Mars Space Flight Facility, School of Earth and Space Exploration, Arizona State University, Tempe, Arizona, USA.

<sup>10</sup>Jet Propulsion Laboratory, California Institute of Technology, Pasadena, California, USA.

<sup>11</sup>Department of Earth and Planetary Sciences, Washington University in St. Louis, St. Louis, Missouri, USA.

<sup>12</sup>Department of Astronomy, Cornell University, Ithaca, New York, USA.

<sup>13</sup>Planetary Science Institute, Tucson, Arizona, USA.

<sup>14</sup>Department of Physics, University of Guelph, Guelph, Ontario, Canada.

<sup>15</sup>Tasmanian ICT Centre, CSIRO, Hobart, Tasmania, Australia.

<sup>16</sup>Lunar Quest Program, NASA Marshall Space Flight Center, Huntsville, Alabama, USA.

### 1. Introduction

[2] The Mars Exploration Rover (MER) Opportunity landed on Meridiani Planum in January 2004 and has since covered a distance of more than 20 km. The Meridiani plains are covered with basaltic sand, with frequent exposures of sulfate-rich outcrop rock and a lag deposit of hematite-rich spherules [e.g., Squyres *et al.*, 2006]. Opportunity investigated the Meridiani lithologic components at numerous locations on the plains and in the inner walls of a number of craters, the largest being Victoria with a diameter of ~800 m [Squyres *et al.*, 2009]. Occasionally, loose rocks with no apparent connection to the ubiquitous outcrop have been encountered. Typically, these rocks have dimensions of several centimeters or more. On the Krumbein  $\phi$  scale [Krumbein and Sloss, 1963], this makes them pebble (4–64 mm) to cobble (64–256 mm) size, but for the sake of simplicity, we refer to these rocks as "cobbles." Cobbles are rare and clusters are observed preferentially near craters. Their investigation is of interest for a number of reasons: cobbles may represent impact ejecta from deeper or more distant geologic units, providing access to materials otherwise inaccessible to the rover. Cobbles may also represent meteoritic material. Presumably, such materials were delivered to their present location through impact events, either as impactors or as secondary impact ejecta. A good

**Table 1.** Overview of Cobbles Discussed in This Paper in Order of Discovery

Name <sup>a</sup>	Sol <sup>b</sup>	Diameter (cm)	Classification
Lion Stone	106	30 by 10	Outcrop fragment
Barberton	123	4	Barberton group
Russett	381	13 by 15	Outcrop fragment
Arkansas	551	5	Arkansas group
Perseverance	554	3	Arkansas group
Antistasi	642	6	Arkansas group
JosephMcCoy	886	<2	Arkansas group
Haiwassee	890	<2	Arkansas group
Santa Catarina	1045	12	Barberton group
Santorini	1741	10	Barberton group
Kos	1880	<2	Arkansas group
Tilos	1880	<2	Arkansas group
Rhodes	1882	3	Arkansas group
Kasos	1886	8	Barberton group
Vail Beach	1974	2	Arkansas group

<sup>a</sup>Names are informal and not officially approved by the International Astronomical Union.

<sup>b</sup>The sol indicates the beginning of investigations with contact instruments.

example is Bounce Rock, a single rock without related fragments, whose composition is similar to basaltic shergottites, a subgroup of meteorites whose origin is thought to be Mars (J. Zipfel et al., Bounce Rock: A basaltic shergottite at Meridiani Planum, Mars, submitted to *Meteoritics and Planetary Science*, 2010). Meteoritic materials often include metallic iron and are thus very sensitive to the presence of water subsequent to their arrival (J. W. Ashley et al., The Scientific Rationale for Studying Meteorites found on Other Worlds, [http://www8.nationalacademies.org/ssbsurvey/DetailFileDisplay.aspx?id=162&parm\\_type=PSDS](http://www8.nationalacademies.org/ssbsurvey/DetailFileDisplay.aspx?id=162&parm_type=PSDS), 2009; J. W. Ashley et al., Evidence for mechanical and chemical alteration of iron-nickel meteorites on Mars: Process insights for Meridiani Planum, submitted to *Journal of Geophysical Research*, 2010). In this paper, we focus on relations between cobbles scattered over a range of several kilometers.

[3] Opportunity is equipped with the Athena Science payload [Squyres et al., 2003]. Two remote sensing instruments are integrated in the Pancam Mast Assembly. The Panoramic Camera (Pancam) provides multispectral imaging capability through 13 “geology” filters in the region from 434 to 1009 nm [Bell et al., 2003]. The Miniature Thermal Emission Spectrometer (MiniTES) covers the infrared wavelength region from 5 to 29.5  $\mu\text{m}$  [Christensen et al., 2003]. Remote sensing data from both instruments provide information on the mineralogy of rocks and soils and often precedes an analysis campaign with the four contact instruments mounted on the Instrument Deployment Device (IDD). The Rock Abrasion Tool (RAT) was designed to expose fresh rock surfaces by grinding away the rock surface and by brushing away dust and soil covering the rock [Gorevan et al., 2003]. The Microscopic Imager (MI) is a fixed focus camera with a field of view (FOV) of 32 by 32 mm with a resolution of 31  $\mu\text{m}/\text{pixel}$  [Herkenhoff et al., 2003]. MI images provide important information about the texture of a sample. Elemental analysis is carried out with the Alpha Particle X-ray Spectrometer (APXS) [Rieder et al., 2003]. The instrument is able to detect elements ranging from sodium (atomic mass = 23) up to bromine (atomic mass = 80). Emitted X-rays are registered by the X-ray detector inside

the sensor head and accumulated in an X-ray energy spectrum. Elements can be identified by their peaks at characteristic energies; elemental abundances can be derived from the peak areas. The Mössbauer spectrometer (MB) provides information about the presence of iron-bearing minerals, iron oxidation states and the distribution of iron among them [Klingelhöfer et al., 2003]. The Mössbauer parameters required for the interpretation of spectra are the isomer shift ( $\delta$ ) and quadrupole splitting ( $\Delta E_Q$ ) for doublets, and  $\delta$ ,  $\Delta E_Q$  and the magnetic hyperfine field ( $B_{\text{hf}}$ ) for sextets. A large number of minerals can be identified through a comparison of cataloged parameters [e.g., Stevens et al., 2002] with parameters determined from MER spectra [e.g., Morris et al., 2006a, 2006b, 2008]. When reconciling APXS and MB data, the different FOV and sampling depths of both instruments have to be taken into account. The MB instrument has a FOV of  $\sim 1.5$  cm and a sampling depth of up to several hundred  $\mu\text{m}$  [Klingelhöfer et al., 2003], whereas the APXS FOV is  $\sim 2.5$  cm for 95% and 1.4 cm for 50% of the signal and the sampling depth is only  $\sim 1$  to 20  $\mu\text{m}$  depending on the element [Brückner et al., 2008].

## 2. Cobble Classification

[4] The 15 cobbles listed in Table 1 were investigated with Opportunity’s contact instruments at 12 different locations between April 2004 and September 2009. We divide the cobbles into three groups, referred to as the “Arkansas Group” and the “Barberton Group,” after the first specimen of each that was encountered by Opportunity, and “Outcrop Fragments.” Pancam images of some representative cobbles are shown in Figure 1. The distribution of cobbles along Opportunity’s traverse is shown in Figure 2; the distribution of the meteorites among those cobbles is discussed in more detail by Schröder et al. [2010]. Two boulders named “Bounce Rock” and “Marquette Island” and four iron meteorites, informally named “Heat Shield Rock,” “Block Island,” “Shelter Island” and “Mackinac Island,” are not further considered in this work because they are significantly larger than cobbles. Bounce Rock was found to be a Martian basalt similar to some basaltic shergottites, a subgroup of the SNC meteorites (named for the three type meteorites Shergotty, Nakhla, and Chassigny) whose origin is thought to be Mars, and is probably crater ejecta (J. Zipfel et al., submitted manuscript, 2010). “Marquette Island” is probably also crater ejecta but not related to meteorites from Mars [Mittlefehldt et al., 2010]. Heat Shield Rock was classified as a IAB complex iron meteorite and given the approved official name “Meridiani Planum” after the location of its find [Connolly et al., 2006]. It has been described in detail by Schröder et al. [2008] and I. Fleischer et al. (New insights into the mineralogy and weathering of the Meridiani Planum Meteorite, Mars, submitted to *Meteoritics and Planetary Science*, 2010). The complete suite of iron meteorites is discussed elsewhere (J. W. Ashley et al., submitted manuscript, 2010; R. Gellert et al., manuscript in preparation, 2010).

[5] Pancam 13-filter spectra were obtained for a much larger number of cobbles than those few investigated with the IDD instruments. Data from more than 200 loose rocks have been assembled in a database [Nuding and Cohen, 2009]. Spectral parameters from 13-filter spectra indicate systematic differences in spectral properties that reveal dif-

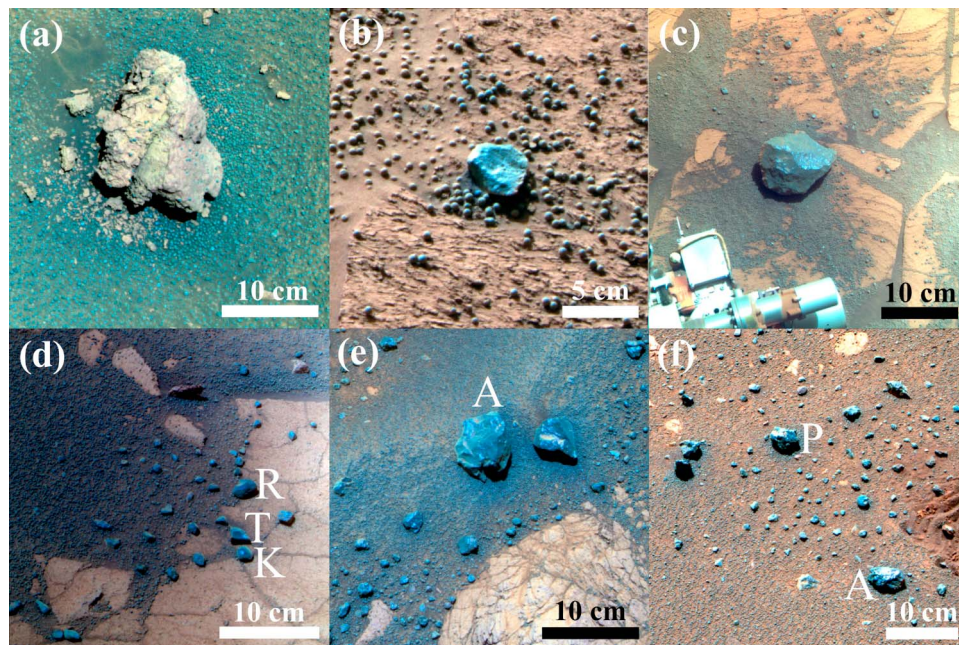


**Figure 1.** Representative false color Pancam images of Meridiani cobbles. (a) Russett; (b) Barberton; (c) Santorini; (d) Rhodes (R), Tilos (T) and Kos (K); (e) Antistasi (A); (f) Perseverance (P) and Arkansas (A). Locations are shown in Figure 2. Image courtesy of NASA/JPL/Pancam.

ferences among cobbles [e.g., *Farrand et al.*, 2008]. Pancam multispectral imaging has proven vital to distinguishing cobbles from outcrop materials, and to selecting which cobbles should be subjected to IDD investigations. However, it is challenging to directly relate data obtained with Pancam and the contact instruments: the instruments have different fields of view and penetration depths, so that some results may be more influenced by clasts and/or discontinuous surface coatings observed in some cobble MI images. Viewing and lighting geometries have a notable effect on Pancam spectra. Figure 3 shows Pancam decorrelation stretches of Russett (outcrop fragment), Antistasi (Arkansas group) and Santa Catarina (Barberton group) that are representative of their types. Figure 4 shows Pancam 13-filter spectra obtained on the three cobbles. The outcrop fragment Russett has spectral properties commensurate with those of Meridiani outcrop. Namely, it is bright compared to soil and appears buff yellow and purple in a stretched composite (left filter numbers 3, 5 and 7; 673, 535, and 432 nm; Figure 3a). Also, it has a higher blue-to-red slope and stronger 535 nm band depth than the darker cobbles. In contrast, the darker cobbles are lower in overall reflectance than outcrop (though relatively brighter at the shortest wavelength 432 nm L7 and 436 nm R1 filters). In stretched L357 composites, these cobbles appear blue. In decorrelation stretch (DCS) versions of these images, the cleanest surfaces of the cobbles are blue, those with some dust contamination appear blue-green (Figure 3b) and surfaces with accumulations of air fall dust are yellow to red (Figure 3c). The cobbles have a low to sometimes negative 535 nm band depth (sometimes a slight 535 nm peak) and generally display a significant 900 nm band depth. Chemically and mineralogically, the dark cobbles are subdivided into two groups, as will be discussed in detail in sections 2.2 and 2.3. The geochemical differences that

distinguish the cobble groups are not overtly manifested in the Pancam multispectral data although there are differences between dark cobbles. Arkansas, Perseverance and others in the vicinity have a shallow and broad long-wavelength absorption centered in some spectra in the 904 nm R5 band, and others in the 934 nm R6 band, with a relative reflectance maximum at 673 nm (Figure 4). In the Jesse Chisholm area cobbles (i.e., close to Erebus Crater), the relative reflectance maximum shifts to 754 nm and the long-wavelength absorption band minimum is more uniform in the 934 nm band. In the Tilos, Kos, and Rhodes spectra, the relative reflectance maximum is at 803 nm with a narrower long-wavelength absorption centered at 934 nm. The cobbles clustering in a cobble field near Santa Catarina (close to the rim of Victoria crater) share a low overall reflectance, low 535 nm band depth, a relative reflectance maximum at 754 nm, and a long-wavelength absorption with a band minimum at 934 nm (Figure 4). However, there are differences in the width of the long-wavelength absorption band which can be characterized by the slope from the 754 to 864 nm bands. *Weitz et al.* [2010] provide more information on Pancam spectral parameters of cobbles.

[6] Based on chemical (APXS) and mineralogical (MB) data, three different cobble groups can be identified. The first group comprises two bright rocks (Lion Stone and Russett) which are compositionally indistinguishable from outcrop rocks and are thus identified as “outcrop fragments.” Dark cobbles can be subdivided into the “Barberton group” and “Arkansas group,” respectively, after the first cobble of each group analyzed by Opportunity. The elemental compositions of cobbles discussed in this paper are summarized in Table 2. Figures 5 and 6 show plots for elemental abundances for all cobble groups in comparison with soils, Meridiani outcrop rocks, and Martian (SNC)

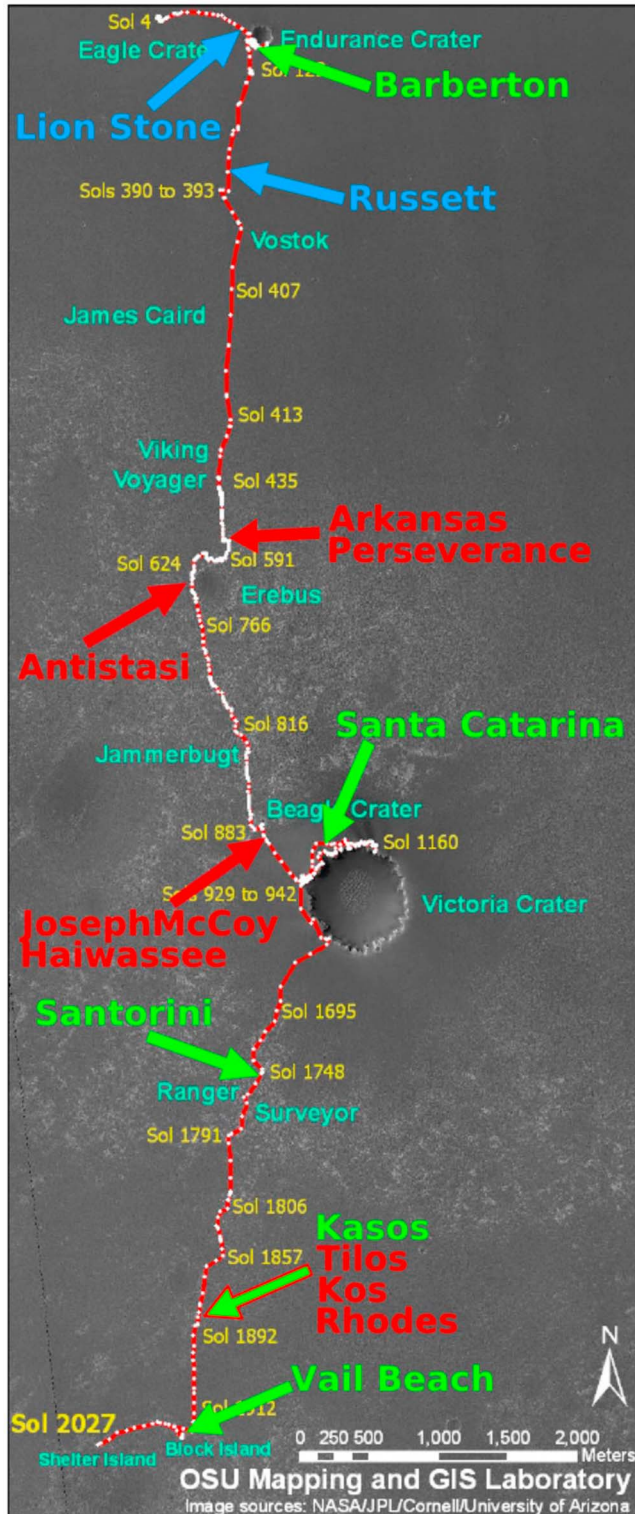


**Figure 2.** The locations of cobbles along Opportunity's traverse, with blue labels for outcrop fragments, green labels for Barberton group, and red labels for Arkansas group. The locations of craters and two of the iron meteorites (Shelter Island and Block Island) are shown in blue-green.

meteorites. Generally, the data for each cobble group form distinct clusters that do not overlap with each other or with soil or outcrop data. An exception is the outcrop fragments, which overlap with data for outcrop rocks.

## 2.1. Outcrop Fragments

[7] Lion Stone sits on the rim of Endurance crater and measures 30 by 10 cm. It is one of many similar rocks encountered on the rims of craters. Undisturbed and abraded spots of the rock's surface were measured and imaged between sols 105 and 108. Russett (~13 by 15 cm) was encountered on the plains ~800 m south of Endurance crater. Only the undisturbed surface of the rock was investigated on sols 380 and 381. In false color Pancam images, both rocks appear bright and red compared to other material in the field of view, including soil, darker cobbles and spherules with a bluish appearance. Pancam spectral parameters of this set of cobbles are also consistent with those of outcrop in terms of their having higher blue-to-red slopes and 535 nm band depths [Farrand *et al.*, 2007; Weitz *et al.*, 2010]. Spherules were also observed, contained within the bulk of each rock, as shown in Figure 7 for the undisturbed surface of Russett. Spherules are typically observed in outcrop rocks, and their occurrence in Russett and Lion Stone is another indication of the connection to outcrop rocks. Both cobbles are indistinguishable from outcrop for all elements (Figures 5 and 6). Compared to other cobbles, their sulfur content is especially high. Their Mössbauer spectra are also typical for outcrop rocks. Figure 8a shows a direct comparison of outcrop fragment spectra and a typical outcrop spectrum; Figure 8b shows the content of iron bearing phases derived from them. Fits yield relative subspectral areas of ~15% divided between olivine and pyroxene, ~25% Fe<sub>3</sub>D<sub>3</sub> (an unassigned ferric phase, cf. Morris *et al.* [2006b]), ~30% jarosite and ~30% hematite. Based on these findings, the Lion Stone and Russett cobbles are identified as outcrop fragments with high confidence. Russett is the only fragment of Meridiani outcrop that Opportunity investigated far from any crater.

[8] Outcrop fragments are larger (>10 cm) than other cobbles (compare Table 1), perhaps because smaller fragments of the comparably soft outcrop rocks are not as long lasting as the other cobble types consisting of harder material.

## 2.2. Barberton Group

[9] Barberton (~4 cm) was encountered on the southern rim of Endurance crater on sol 121. Seven kilometers further south, Santa Catarina (14 by 11 cm) was found in a cobble field close to the northern rim of Victoria Crater. Between sols 1045 and 1048, MI images, APXS, and Mössbauer spectra were obtained on the undisturbed, but relatively dust-free surface of the Santa Catarina. Schröder *et al.* [2008] have provided a detailed description of Barberton and Santa Catarina. From sol 1713 to sol 1749, ~800 m south of Victoria crater, the ~10 cm cobble Santorini was analyzed [Schröder *et al.*, 2009]. Kasos (~8 cm) was encountered ~1.5 km south of Victoria crater, in close proximity to the Arkansas group cobbles Tilos, Kos, and Rhodes. The undisturbed surface of Kasos was investigated between sols 1886 and 1890. None of the Barberton group cobbles were brushed or abraded with the RAT because of their small size and unfavorable geometry. In true and false color Pancam images, all these

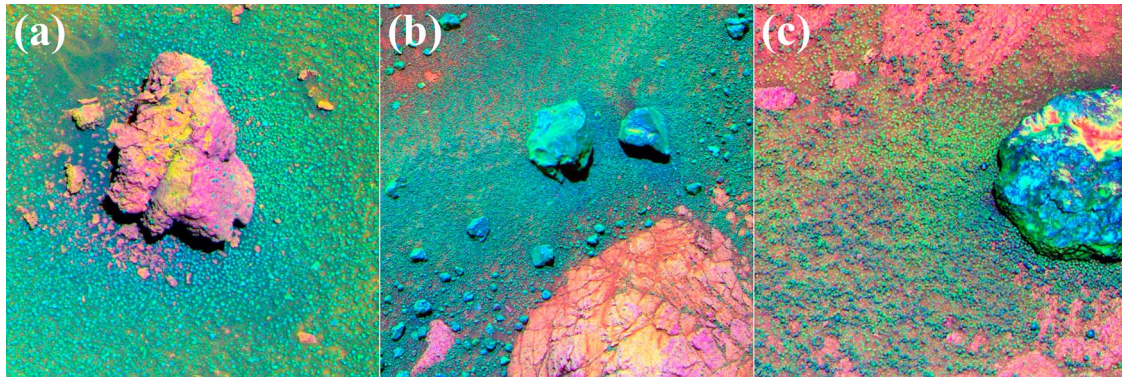


**Figure 3.** Decorrelation stretches showing the (a) outcrop fragment Russett, (b) Arkansas group cobble Antistasi, and (c) Barberton group cobble Santa Catarina.

cobbles appear dark compared to outcrop and soil in the field of view (Figures 1b–1d). Figure 9 shows MI images of the two Barberton group cobbles Santa Catarina and Santorini. Santa Catarina MI images clearly show several clasts, suggesting a brecciated texture (compare also *Schröder et al.* [2008, Figure 11]). Compared to Santa Catarina, Santorini does not look brecciated; its surface appears to be clean from dust and partly glassy and lustrous. Barberton is partly coated by dust masking diagnostic textures, and the surface is somewhat pitted. The surface of Kasos is cleaner, showing a clastic texture with mostly subrounded clasts. Glints of sunlight suggest a glassy luster, perhaps resulting from a coating.

[10] APXS spectra were obtained of one spot each on Barberton, Santa Catarina, and Kasos, and two spots on Santorini. Elemental trends are shown in Figures 5 and 6 in comparison with Meridiani soils, outcrop rocks, other cobbles, and SNC meteorites. SNC meteorites are inferred to have originated from Mars [e.g., *McSween et al.*, 1979; *Nyquist et al.*, 1979; *Walker et al.*, 1979; *Wasson and Wetherill*, 1979; *Bogard and Johnson*, 1983; *Treiman et al.*, 2000]. They are included in all these plots because they allow comparison of all Meridiani cobbles to Martian materials excavated by impact events.

[11] The P/Al ratio is characteristic for most SNCs. These elements are both incompatible in mafic igneous systems, and their correlation in SNC meteorites is a result of igneous fractionation in Martian magmas. Meridiani soils and outcrops depart from the P–Al trend line indicating chemical weathering and/or physical transport have separated the mineral hosts—phosphates and feldspars—from the original igneous parents. The Barberton group cobbles follow the SNC P–Al trend. The Meridiani soils and outcrops show a strong trend in the Ca–Al plot that is distinct from that of SNC meteorites. Barberton group cobbles plot close to the Ca–Al trend line defined by Meridiani samples, and distinct from the SNC meteorites. SNC meteorites show a good correlation for Ti and Al, which can also be observed for all Meridiani outcrops. The Barberton group Ti–Al concentrations plot below the correlation line, but are similar to some SNC meteorites. The SNCs span a wide field in the Mg/Si versus Al/Si diagram shown in Figure 5. Some SNCs follow the Mars mantle–crust fractionation line (bold line) [e.g., *Dreibus et al.*, 2003]. Other SNCs seem to follow a different evolution line (dashed line). Barberton group cobbles plot

close to the Mars fractionation line. In the Ca–K plot (Figure 6), Barberton group cobbles span the concentrations between the SNCs and the Meridiani samples. The Barberton cobble plots closest to other Meridiani materials, probably due to soil in the FOV. Cl and S concentrations are similar for soils and most cobbles, with the lowest values for Barberton group cobbles. The concentrations of both elements are significantly higher in outcrop rocks, and significantly lower in SNC meteorites. Barberton group cobbles are among the samples with the highest Cr contents observed at Meridiani Planum and plot on the Mg–Cr correlation line for SNCs (Figure 6). SNCs have variable olivine contents, with very high contents for chassignites (available at <http://curator.jsc.nasa.gov/antmet/mmc>) and Ni can be incorporated in olivine during crystallization, which is the cause of the Ni–Mg correlation observed for SNC meteorites. The overall Ni and Mg concentrations are tightly clustered for Meridiani Planum materials except for the Barberton group cobbles. Their Ni concentrations range between ~1500 and 5000  $\mu\text{g/g}$  and their Mg contents are about twice that of soils and outcrops. The extremely high Ni contents of the Barberton group cobbles and their deviations from SNC compositions point to a meteoritic (i.e.,

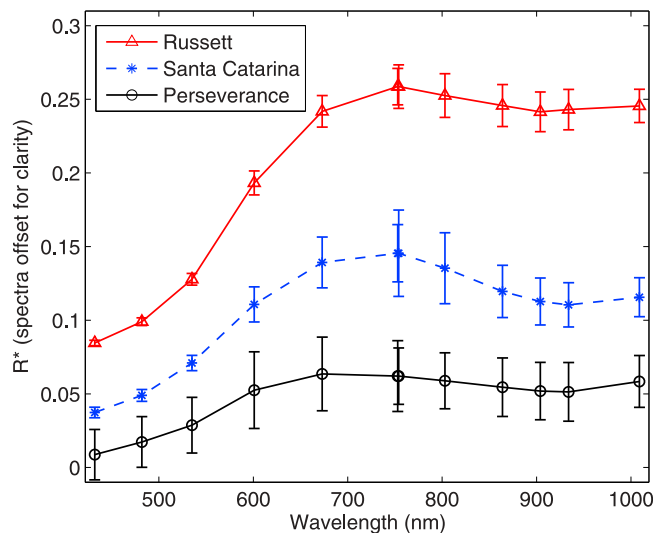


**Figure 4.** Pancam 13-filter spectra for the three cobbles shown in Figure 3.

**Table 2.** Elemental Composition of Cobbles<sup>a</sup>

Sol	Sample	Na	SE	Mg	SE	Al	SE	Si	SE	P	SE	S	SE	Cl	SE	K	SE
108	Lion Stone	1.28	0.23	5.31	0.09	3.29	0.06	17.4	0.18	0.443	0.038	9.15	0.09	0.913	0.021	0.486	0.051
122	Barberton	1.31	0.25	8.92	0.14	3.28	0.09	20.7	0.24	0.289	0.038	2.23	0.04	0.599	0.022	0.242	0.051
381	Russett	1.37	0.15	4.31	0.06	3.60	0.05	18.0	0.17	0.459	0.035	8.34	0.08	0.944	0.020	0.476	0.051
552	Arkansas	1.46	0.12	4.77	0.05	4.36	0.04	19.9	0.13	0.554	0.033	3.96	0.04	1.314	0.019	0.459	0.049
554	Perseverance	1.12	0.14	4.30	0.06	4.68	0.06	20.6	0.18	0.528	0.036	2.77	0.04	0.949	0.021	0.454	0.052
642	Antistasi	1.87	0.13	4.60	0.05	6.05	0.06	22.1	0.17	0.476	0.032	1.49	0.02	0.532	0.011	0.373	0.048
886	JosephMcCoy	1.76	0.17	4.54	0.07	5.22	0.07	20.9	0.17	0.443	0.038	1.96	0.04	0.674	0.024	0.396	0.054
890	Haiwassee	1.59	0.17	4.34	0.07	4.84	0.07	20.4	0.22	0.443	0.037	2.40	0.04	0.817	0.023	0.389	0.053
1046	Santa Catarina	1.12	0.26	10.88	0.12	2.30	0.05	20.6	0.19	0.265	0.031	2.04	0.03	0.618	0.014	0.119	0.045
1745	Santorini1	1.11	0.24	10.73	0.11	2.35	0.05	20.6	0.20	0.256	0.030	1.56	0.02	0.529	0.012	0.118	0.045
1747	Santorini2	1.06	0.27	11.86	0.13	2.08	0.05	20.9	0.23	0.236	0.030	1.36	0.02	0.507	0.013	0.089	0.044
1886	Kasos	1.18	0.15	11.01	0.09	2.26	0.04	20.4	0.14	0.238	0.029	2.20	0.03	0.428	0.010	0.122	0.045

Sol	Sample	Ca	SE	Ti	SE	Cr	SE	Mn	SE	Fe	SE	Ni	SE	Zn	SE	Br	SE
108	Lion Stone	3.60	0.03	0.460	0.046	0.126	0.022	0.224	0.009	11.1	0.08	572	52	415	19	268	20
122	Barberton	3.16	0.04	0.305	0.043	0.342	0.030	0.280	0.015	15.4	0.13	1639	89	207	25	47	21
381	Russett	3.91	0.03	0.482	0.041	0.134	0.022	0.236	0.009	12.0	0.08	628	51	585	21	60	16
552	Arkansas	5.18	0.03	0.567	0.039	0.178	0.021	0.254	0.007	13.5	0.06	539	45	418	15	110	16
554	Perseverance	4.89	0.04	0.560	0.043	0.154	0.025	0.237	0.010	15.9	0.09	508	65	327	24	79	19
642	Antistasi	4.95	0.03	0.650	0.040	0.166	0.021	0.233	0.007	12.9	0.06	899	49	189	12	35	14
886	JosephMcCoy	4.78	0.05	0.622	0.049	0.196	0.028	0.238	0.013	15.6	0.09	807	81	263	29	37	20
890	Haiwassee	4.81	0.05	0.570	0.047	0.159	0.027	0.238	0.013	16.5	0.13	566	69	282	25	64	21
1046	Santa Catarina	2.45	0.02	0.142	0.035	0.420	0.025	0.292	0.009	16.0	0.10	3207	76	164	13	59	16
1745	Santorini1	2.33	0.02	0.184	0.035	0.415	0.024	0.290	0.009	17.2	0.11	3255	76	128	12	22	15
1747	Santorini2	2.09	0.02	0.141	0.035	0.423	0.024	0.304	0.009	16.3	0.11	4979	91	120	12	20	15
1886	Kasos	2.14	0.02	0.137	0.034	0.375	0.022	0.304	0.008	16.3	0.06	2722	65	88	9	99	15

<sup>a</sup>Sol refers to APXS measurement. Concentrations are given in weight % of element or parts per million for Ni, Zn, and Br. Error (SE) is absolute statistical error (2 sigma error for the precision of the value). Values for the Arkansas group cobbles Tilos, Kos, Rhodes, and Vail Beach are preliminary and therefore not listed. A detailed analysis will be presented in a future manuscript (R. Gellert et al., manuscript in preparation, 2010).

non-Martian) origin. The overall chemical composition of Barberton group cobbles is most consistent with mesosiderite silicate clasts [Schröder et al., 2008].

[12] A direct comparison of the four Barberton group Mössbauer spectra is shown in Figure 10a, the similarities between the spectra are evident. Figure 10b shows a comparison of the contents of iron bearing phases in the rocks, and the fits are shown in Figure 11. The plots are derived from simultaneous fits with the MERFit program [Agresti and Gerakines, 2009]. These simultaneous fits were carried out because of the similarities between all spectra. This approach provides the possibility to establish parameter relations between separate spectra. Mössbauer parameters for any given mineral phase can be set equal for all spectra of the data set. Each individual spectrum is preserved in the fit. The fits for Barberton group cobbles are derived from a model including olivine, pyroxene, kamacite ( $\alpha$ -Fe,Ni), troilite (FeS) and nanophase ferric oxide (npOx, a generic name for iron oxides or oxyhydroxides with particle sizes in the nanometer range that are superparamagnetic at the temperature of observation, e.g., hematite ( $\alpha$ -Fe<sub>2</sub>O<sub>3</sub>), maghemite ( $\gamma$ -Fe<sub>2</sub>O<sub>3</sub>) or goethite ( $\alpha$ -FeOOH)) [e.g., Morris et al., 2006a]. Kamacite and troilite are typically present in meteorites. The Mössbauer parameters of both phases were set constant in all fits because of their comparably small subspectral areas. Parameters for kamacite and troilite were obtained from a specimen of the Mundrabilla meteorite measured at a temperature of ~235 K (I. Fleischer et al., submitted manuscript, 2010). Mössbauer parameters and subspectral areas are given in Table 3, based on independent fits by three of us to ensure consistency of the derived values.

[13] Barberton, Santa Catarina and Santorini have spectra with more Fe from olivine than from pyroxene, with the

opposite for Kasos. The simultaneous fit demonstrates that the spectra obtained on Barberton and Santorini show the presence of kamacite and troilite, while the Santa Catarina spectrum shows almost exclusively troilite. These results are consistent with spectral interpretations previously published by Morris et al. [2006b] and Schröder et al. [2008]. The Kasos spectrum is characterized by poorer counting statistics compared to the other cobbles because of decreased activity of the Mössbauer source at the time of the measurement (sol ~1890), but it is in agreement with the presence of both kamacite and troilite.

[14] These results show that Barberton group cobbles are fundamentally different from all other materials investigated at Meridiani Planum. Genetic associations of Santa Catarina with additional cobbles in its vicinity are implied by MiniTES data [Ashley et al., 2009]. A detailed discussion of possible pairing of the Barberton group cobbles and resulting implications is provided by Schröder et al. [2010].

### 2.3. Arkansas Group

[15] Three cobbles were investigated close to Erebus crater (Figure 2). Arkansas (~5 cm) and Perseverance (~3 cm) were investigated between sols 551 and 554, and Antistasi (~5 cm) between sols 641 and 645. JosephMcCoy and Haiwassee (sol 886–890) are both small (<2 cm) cobbles encountered in the “Jesse Chisholm area,” a dark mound close to Beagle crater (~1.5 km south of Erebus crater). Tilos, Kos and Rhodes were encountered ~1.5 km south of Victoria crater between sols 1880 and 1882, just a few meters from the Barberton group cobble Kasos. The small (~2 cm) cobble Vail Beach was investigated on sol 1974, ~4 km south-southwest of Victoria crater. In false color and true color Pancam images, Arkansas group cobbles appear dark (comparable to Barberton group

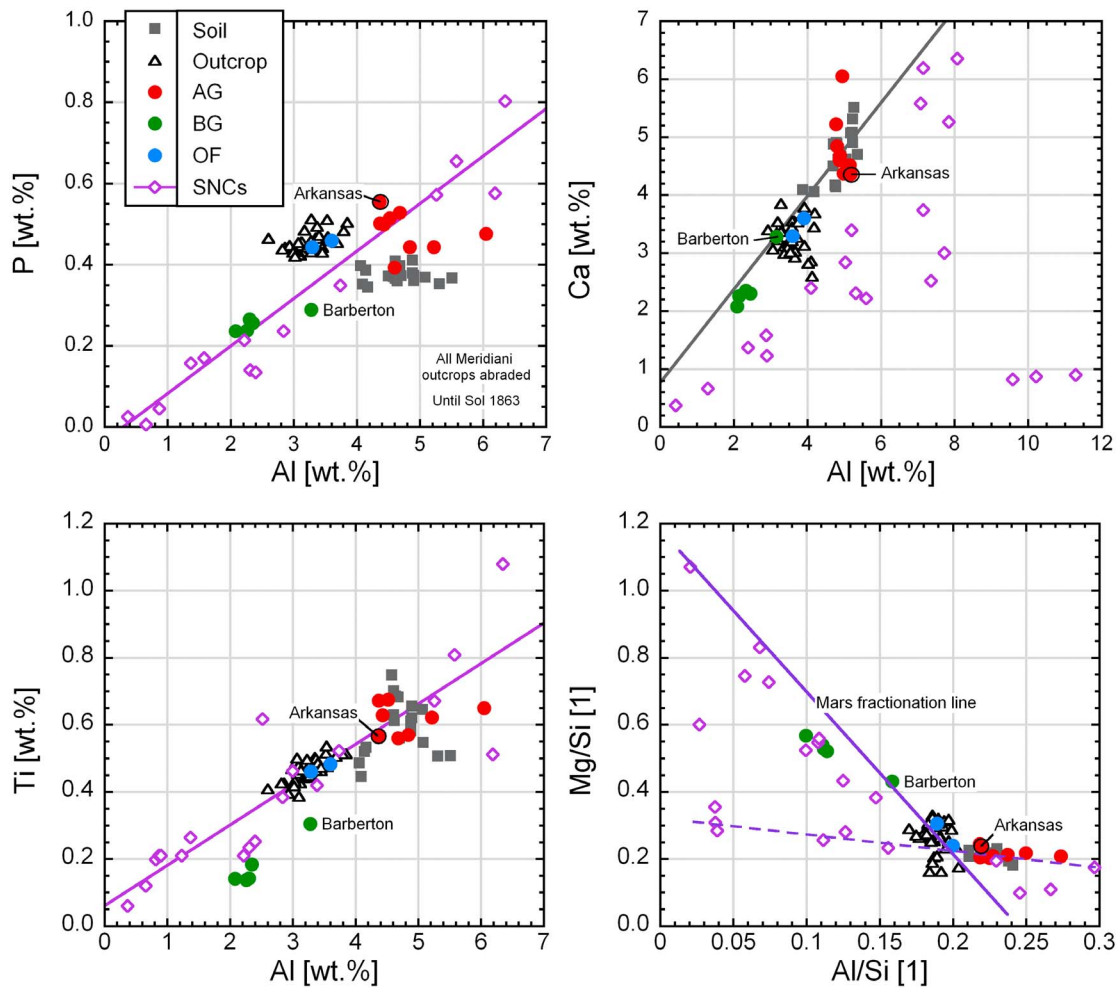


**Figure 5.** Composition of cobbles compared to Meridiani outcrop, soil, and SNC meteorites for P versus Al, Ca versus Al, Ti versus Al, and Mg/Si versus Al/Si. Outcrop fragments (OF) are indistinguishable from other outcrop rocks; Barberton group cobbles (BG) are clearly different from any other material; Arkansas group cobbles (AG) appear compositionally close to soil for a number of elements. For the P-Al and Ti-Al plots, correlation lines are calculated for the SNC samples. In the Ca-Al plot, a trend line is derived from soil samples.

cobbles) with irregular shapes. Microscopic images show nearly dust-free surfaces with heterogeneous textures. Two representative MI images obtained on JosephMcCoy and Perseverance are shown in Figure 12. Brighter and darker areas are clearly visible. Both cobbles appear to consist of large, subangular brighter grains in a darker matrix [Herkenhoff *et al.*, 2008]. It is also possible that the brighter areas result from a discontinuous coating on their surfaces, rather than internal textural differences.

[16] Compared to Barberton group cobbles, Arkansas group cobbles are generally high in Al, P, K, Ca and Ti; and low in Ni, Mg and Cr. The plots shown in Figures 5 and 6 indicate that there is a close relationship between soils and the Arkansas group cobbles. Compared to outcrop and other cobbles, Ti and Al concentrations are high for soils and Arkansas group cobbles. Arkansas group cobbles have Ca and Al concentrations very similar to those of Meridiani soils; and the Ni and Mg contents are also in a similar range. The Mg/Si versus Al/Si plot (Figure 5) also emphasizes the similarity between soils and Arkansas group cobbles com-

pared to outcrop rocks. SNC meteorites cover a wider range. The Ca-K plot (Figure 6) shows that, in contrast to the SNCs, the incompatible element K is enriched in all soils, outcrops, and the Arkansas group cobbles. For P, some Arkansas group cobbles are similar to soils, but many have higher P contents that are more similar to those of outcrop rocks. This fact points to different P mobilities and thus to different formation processes of soil and cobbles. Outcrop rocks have high concentrations of Cl and S. For these two elements, Arkansas group cobbles generally plot close to the soil field. The Arkansas cobbles are an exception; it is more similar to outcrop, likely because of a significant contribution to its makeup from outcrop material. The Cr concentrations of Arkansas group cobbles are intermediate between those of soils and outcrop rocks.

[17] The cobbles Tilos, Kos and Rhodes did not completely fill the APXS field of view, so that underlying outcrop or soil in the instrument FOV likely contributed to the elemental concentrations. However, with their comparably low concentrations of Ni, Cr, and Mg, these cobbles are

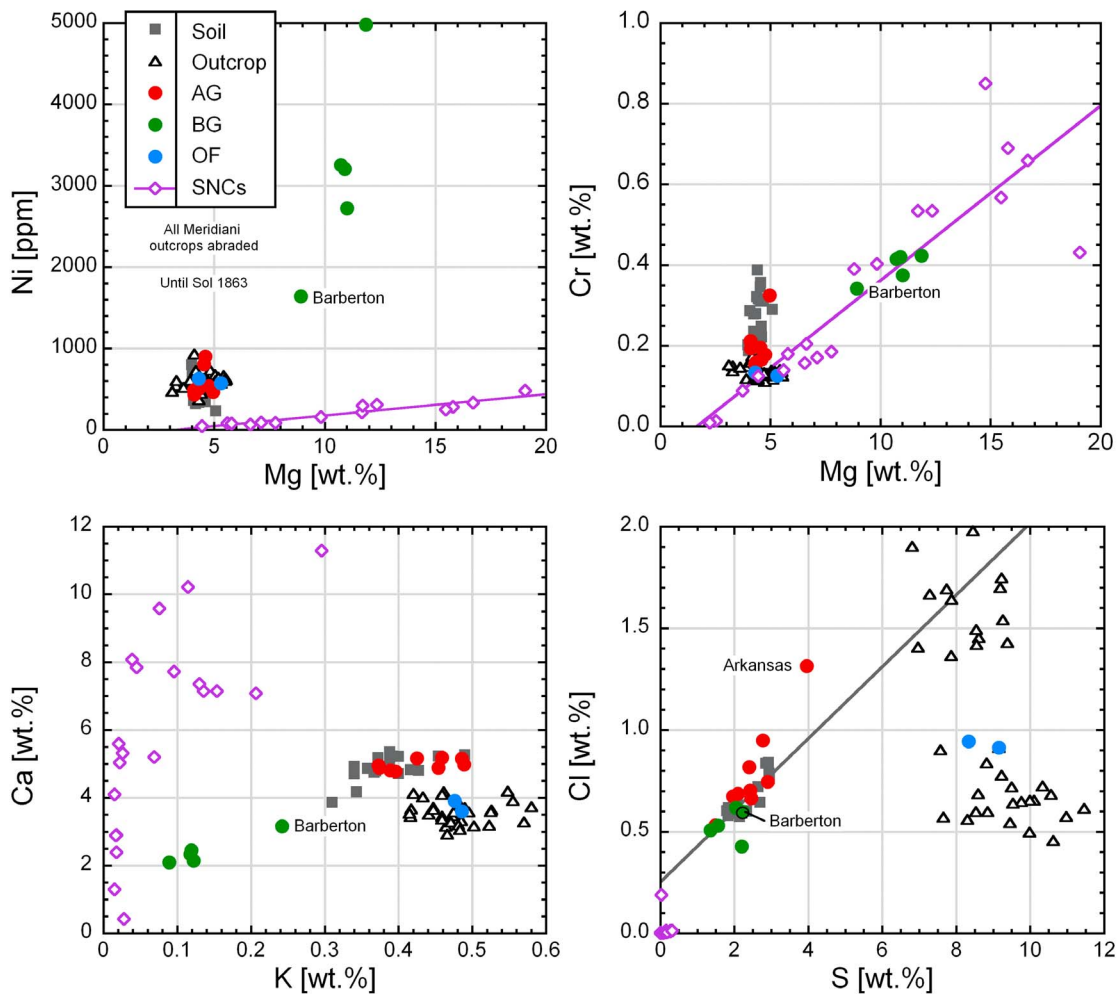


**Figure 6.** Composition of cobbles compared to outcrop, soil, and SNC meteorites for Ni and Cr versus Mg, with correlation lines for the SNCs. No trend line was found for the Ca-K plot. In the Cl-S plot, a trend line is derived based on the Meridiani soil samples. Some outcrop rocks scatter around this line, while others show a strong depletion in Cl compared to S.

clearly not specimens of the Barberton group. The concentrations of Al, P, K, Ca and Ti are comparably high, characteristic for Arkansas group cobbles.

[18] Mössbauer spectra were measured on Arkansas, Antistasi, and JosephMcCoy. The Antistasi and JosephMcCoy Mössbauer spectra are very similar to each other. The Arkansas spectrum has a larger ferric component and also shows similarities to typical Meridiani outcrop spectra, with the obvious exception that the hematite sextet signature is less pronounced in the Arkansas spectrum. A direct comparison of the spectra is shown in Figure 13a, along with contents of iron-bearing phases in the rocks shown in Figure 13b.

[19] Satisfactory fits of all spectra were obtained by using a model with three ferrous doublets corresponding to the basaltic minerals olivine, pyroxene and ilmenite, one ferric doublet and one sextet representing hematite. There is no evidence for kamacite or troilite in the Arkansas group cobbles in the Mössbauer spectra. All three spectra, with phases derived from a simultaneous fit, are shown in Figure 14. Mössbauer parameters and subspectral areas (Table 4) are

based on independent fits by three of us to ensure consistency of the derived values. In the simultaneous fit, ilmenite parameters were fixed to values from [Morris *et al.*, 2006a], reported for ilmenite-bearing rocks encountered by the MER Spirit in Gusev crater. The hematite center shift was fixed to 0.37 mm/s because of the low subspectral area of hematite.

[20] Olivine and pyroxene occur in all basaltic soils and most rocks at both landing sites; and dominate the Mössbauer spectra of Antistasi and JosephMcCoy. Ilmenite has previously not been reported at Meridiani. While the subspectral areas for ilmenite are within uncertainty of zero, the presence of ilmenite in Arkansas group cobbles is consistent with the Ti concentrations in these rocks (Figure 5). The Ti concentrations are equivalent to Ti concentrations in typical Martian basaltic soils, which contain titanomagnetite [Morris *et al.*, 2008]. A signature consistent with titanomagnetite is not observed in Mössbauer spectra from Arkansas group cobbles. Hematite, a constituent of Meridiani outcrop, is clearly present in the Arkansas spectrum and potentially also in the JosephMcCoy spectrum, with poorer counting statistics. The quadrupole splitting of the ferric



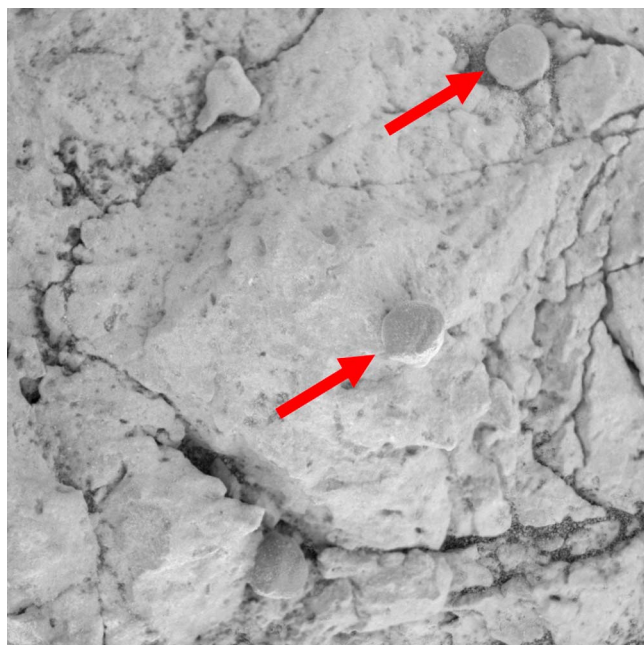


**Figure 7.** Merge of four radiometrically calibrated MI images of target “Eye” on undisturbed surface of outcrop fragment “Russett,” taken on sol 381 when the target was fully shadowed. Area shown is  $\sim 3$  cm square. Embedded spherules (arrows) are clearly visible. Image courtesy of NASA/JPL/MI.

doublet from Arkansas group spectra is larger compared to npOx from soil and most other rocks from both MER landing sites [Morris *et al.*, 2006a, 2006b], and smaller compared to that of jarosite in Meridiani outcrop spectra. Similar Mössbauer parameters were derived for npOx from spectra obtained on rocks encountered by Opportunity’s twin rover Spirit in the Columbia Hills [Morris *et al.*, 2006a, 2008]. This assignment appears reasonable for the ferric doublet observed in spectra of the Arkansas cobble group, although the history of both rock groups is entirely different. The large quadrupole splitting may also reflect a contribution from jarosite in addition to npOx. However, it is not

possible to resolve two ferric doublets in a consistent way for all Arkansas group spectra.

[21] The general texture and dark color of all Arkansas group cobbles show that they are clearly not rocks dominated by unaltered outcrop fragments. The high S content measured in the Arkansas cobble suggests a relation to outcrop, such as the presence of small outcrop fragments in a darker matrix.

[22] The differences of the npOx Mössbauer parameters between spectra from Arkansas group cobbles on the one hand, and spectra from soil or dust on the other hand exclude the possibility that the npOx signature stems from dust coatings on the cobble surface.

[23] The Mössbauer spectra of Arkansas group cobbles show substantially greater variability than those of the other cobble groups. This variability may result in part from the centimeter-scale mineralogical heterogeneity in Arkansas rocks. The field of view of the APXS is  $\sim 2.5$  cm in diameter, while that of the Mössbauer spectrometer is smaller (1.5 cm). The clast-in-matrix texture of these rocks, as seen in MI images (Figure 12), hints at significant centimeter-scale compositional heterogeneity. Both instruments may have incompletely sampled this heterogeneity and hence show significant sample-to-sample variability, where APXS spectra may be at least somewhat more representative of the average composition.

#### 2.4. Cobble Classification Based on Principal Component Analysis of APXS Data

[24] Principal Component Analysis (PCA) of APXS data brings insight regarding the classification of the cobbles on the basis of their chemical compositions. Through a change of reference frame, from the initial basis of elemental abundances to the new basis of the Principal Components (PC), PCA allows the data to be plotted with fewer axes in the new PC space. This highlights compositional variance in a way that is not necessarily apparent on simpler binary element-element or oxide variation diagrams. The approach is described in detail by Tréguier *et al.* [2008]. We performed PCA using chemical compositions based on the 16 chemical elements usually measured by APXS (compare Table 2), including all Meridiani outcrop rocks, soils

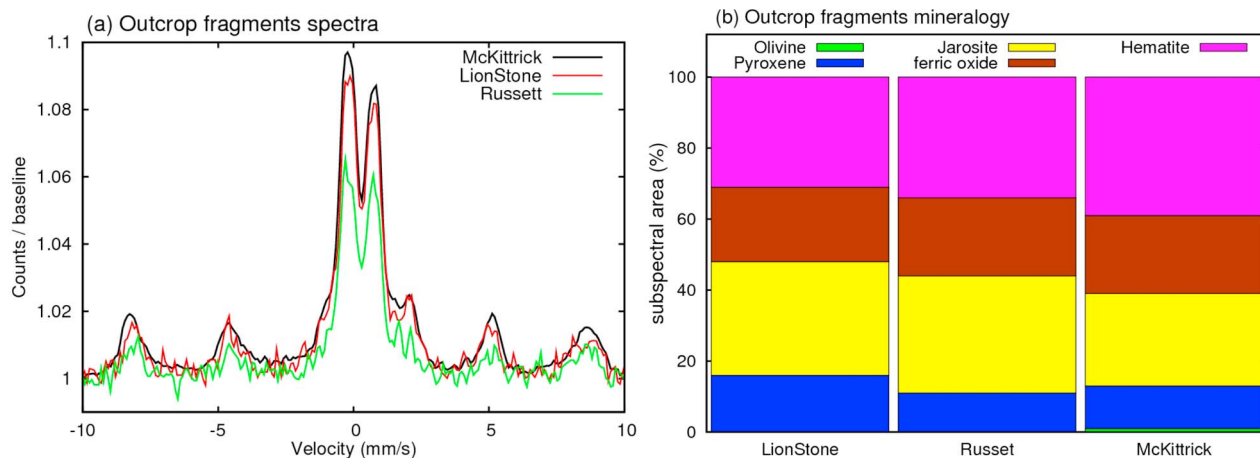


**Figure 8.** (a) Mössbauer spectra of the two outcrop fragments “Lion Stone” and “Russett” are practically identical to a typical outcrop spectrum (McKittrick). (b) The derived mineralogy is also very similar.

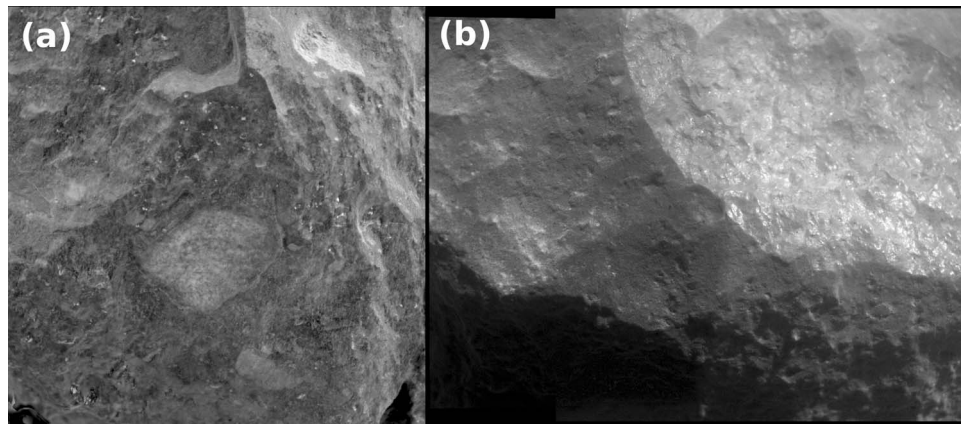


**Figure 9.** (a) Merge of seven radiometrically calibrated MI images of “Santa Catarina” taken on sol 1055 when target was fully shadowed. Area shown is  $\sim 3$  cm square. Clasts are clearly visible. (b) MI mosaic of “Santorini” taken on sol 1747. Area shown is  $\sim 3$  cm high, illumination from upper right. The surface appears partly lustrous.

(including spherule-rich targets) and 13 cobbles (including Bounce Rock). The cobbles Tilos, Kos and Rhodes were not plotted because of their small size and therefore unknown proportion of soil in the field of view.

[25] In this analysis, all abundances were standardized to a mean of 0 and a standard deviation of 1 in order to place greater weight on relative variations in concentration rather than absolute values of abundance. The scatterplot in Figure 15 shows data in the plane of the two first principal components, representing 54.5% of total data variance.

[26] This analysis clearly supports the interpretation of Lion Stone and Russett as outcrop fragments as they plot within the bulk of Meridiani abraded outcrop measurements. Arkansas and Perseverance appear compositionally similar to regular undisturbed outcrop rocks, which represent a mixture of basaltic soil, dust and outcrop with surface coatings. The other Arkansas group cobbles differ more from the bulk of outcrop samples. The three cobbles Vail Beach, Haiwassee and Joseph McCoy appear compositionally similar to each other, whereas Antistasi appears com-

positionally different from other Arkansas group cobbles. The spherule-rich target Berry Bowl (outcrop with hematitic spherules collected in a surface hollow) plots close to Arkansas group cobbles, consistent with the detection of hematite in Arkansas and Joseph McCoy. Barberton group cobbles are all different from the rest of Meridiani samples (rocks or soils). Santa Catarina, Kasos and Santorini form a relatively compact cluster. The Barberton cobble is the smallest rock piece of the group and probably did not completely fill the field of view of the APXS instrument. This is likely the reason that in all elemental plots (Figures 5 and 6) Barberton is closer to soils than other Barberton group cobbles. This could indicate that Barberton is a mixture of Santa Catarina-like material with some amount of soil. A subtraction of a soil component as was done by Schröder *et al.* [2008] moves Barberton toward the other three cobbles of that group in PC space. Three of the Arkansas Group cobbles included in the PCA have a diameter of less than 2 cm, less than the FOV of the APXS ( $\sim 2.5$  cm). These three, Joseph McCoy, Haiwassee, and Vail

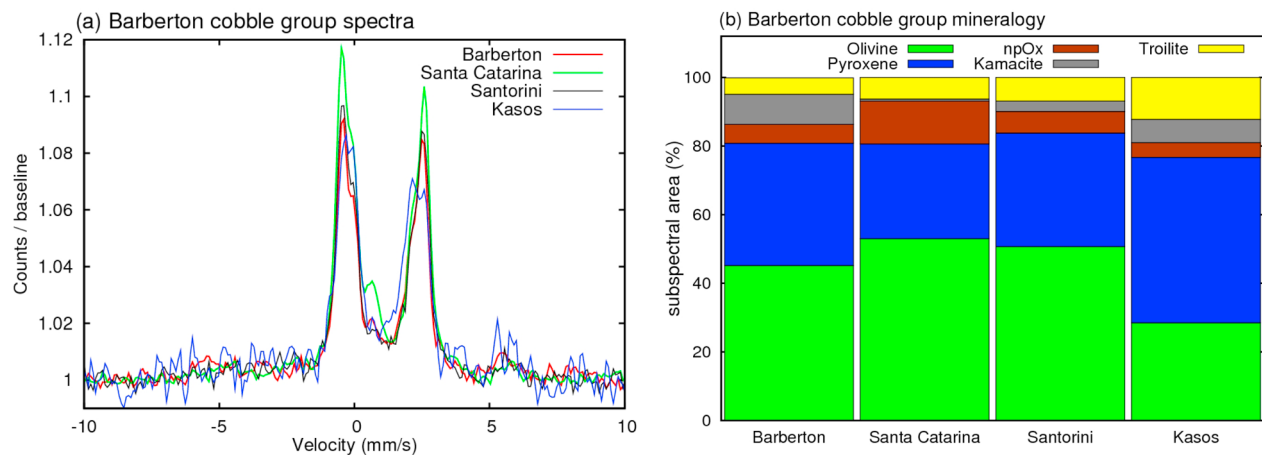


**Figure 10.** (a) The “Barberton group cobbles” (Barberton, Santa Catarina, Santorini, and Kasos) show very similar Mössbauer spectra dominated by the basaltic minerals olivine and pyroxene. (b) Additional contributions from kamacite and troilite are present.

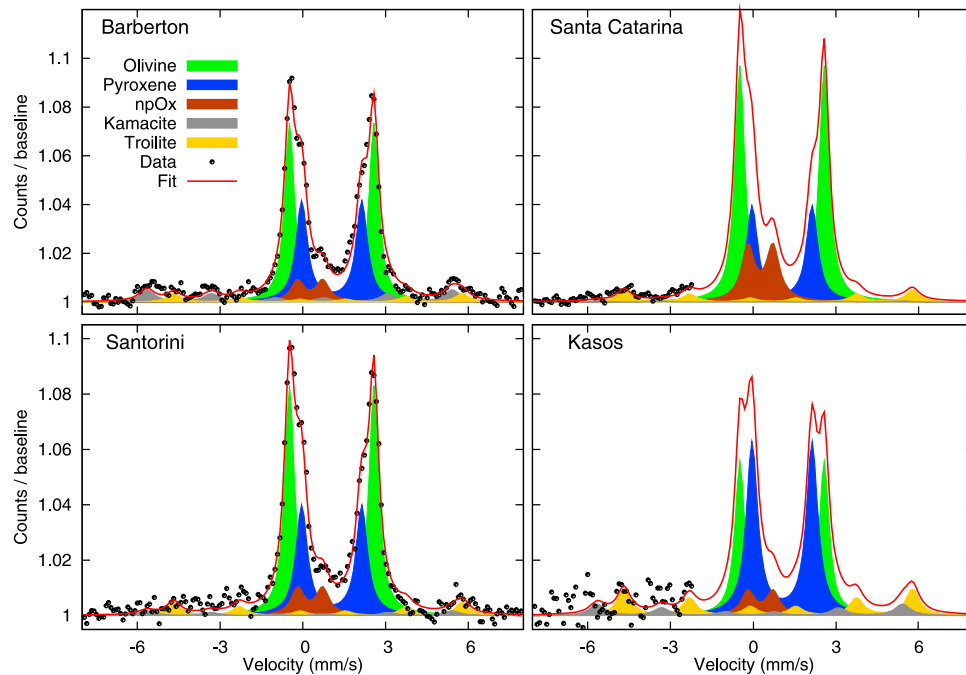


**Figure 11.** Barberton group Mössbauer spectra with iron-bearing components derived from a simultaneous fit of all spectra.

Beach, fall clearly in the field of the soils (Figure 15) pointing to a contribution of the underlying soil to the APXS analysis. Antastasi, which is somewhat larger (6 cm in diameter), seems to have a soil contribution, too. Results from PCA of APXS data support the interpretations and cobble classification based on Mössbauer mineralogical data and APXS elemental weight ratios.

### 3. Possible Origins of Barberton and Arkansas Group Cobbles

[27] Cobbles have been observed along Opportunity's traverse since Eagle crater. Cobbles that appear related based on Mössbauer-determined mineralogy and APXS-determined composition are separated by several kilometers. Cobbles appear more concentrated near impact craters and in some cases, a direct connection between dark cobbles and craters can also be inferred [Golombek *et al.*, 2010]. Several

options for cobble origins have been identified by Jolliff *et al.* [2006]. Cobbles may be (1) fragments of meteorites, (2) fragments of ejecta from impacts elsewhere on Mars delivered to the local region, many of which may have formed secondary craters, (3) locally derived ejecta from outcrop rocks, (4) resistant material eroded from the sulfate-rich outcrop, e.g., rinds and fracture fillings, (5) erosional remnants of a layer that once lay above the presently exposed outcrops, (6) erosional remnants of a deeper layer within the underlying but local stratigraphy, brought to the surface as impact ejecta, (7) impact melts of the outcrop lithology or a mixture of the outcrop lithology and underlying strata.

[28] The clear enrichment of Ni in all Barberton group cobbles along with the detection of kamacite and troilite and the clast-in-matrix texture suggests a meteoritic origin of this cobble group (option 1). The overall chemistry and mineralogy is consistent with a mesosiderite silicate clast

**Table 3.** Mössbauer Parameters and Subspectral Areas for Barberton Group Cobbles<sup>a</sup>

Cobble	Olivine			Pyroxene			npOx <sup>b</sup>			Kamacite <sup>c</sup>				Troilite <sup>c</sup>			
	$\delta^d$ (mm/s)	$\Delta E_Q$ (mm/s)	A (%)	$\delta$ (mm/s)	$\Delta E_Q$ (mm/s)	A (%)	$\delta$ (mm/s)	$\Delta E_Q$ (mm/s)	A (%)	$\delta$ (mm/s)	$\Delta E_Q$ (mm/s)	$B_{hf}$ (T)	A (%)	$\delta$ (mm/s)	$\Delta E_Q$ (mm/s)	$B_{hf}$ (T)	A (%)
Barberton	1.16	3.03 <sup>e</sup>	48	1.15	2.15 <sup>e</sup>	32	0.38	0.88 <sup>e</sup>	6	0.01	-0.02	34.5	11	0.75	-0.17	31.3	3
Santa Catarina	1.16	3.06	52	1.17	2.18	26	0.36 <sup>e</sup>	0.93 <sup>e</sup>	14	0.01	-0.02	34.5	1	0.75	-0.17	31.8	6
Santorini	1.16	3.04 <sup>e</sup>	53	1.17	2.15 <sup>f</sup>	28	0.39 <sup>e</sup>	0.97 <sup>f</sup>	8	0.01	-0.02	34.5	2	0.74	-0.17	31.6	9
Kasos	1.17	3.03 <sup>e</sup>	32	1.16 <sup>e</sup>	2.16 <sup>f</sup>	41	0.39 <sup>e</sup>	0.97 <sup>f</sup>	8	0.00	-0.01	34.6	5	0.74	-0.17	31.6	14

<sup>a</sup>Uncertainties for parameters are  $\pm 0.02$  mm/s ( $1\sigma$  deviation) for  $\delta$  and  $\Delta E_Q$  and  $\pm 0.8T$  for  $B_{hf}$  unless indicated otherwise. Uncertainties for subspectral areas for Barberton, Santa Catarina and Santorini are  $\pm 2\%$  (absolute) and  $\pm 4\%$  for Kasos.

<sup>b</sup>Abbreviation npOx: nanophase ferric oxide.

<sup>c</sup>Kamacite and Troilite parameters were constrained to values obtained from a specimen of the Mundrabilla meteorite measured at  $\sim 235$  K.

<sup>d</sup>The Mössbauer center shift  $\delta$  is given relative to  $\alpha$ -Iron.

<sup>e</sup>Uncertainty  $\pm 0.05$  mm/s.

<sup>f</sup>Uncertainty  $\pm 0.07$  mm/s.

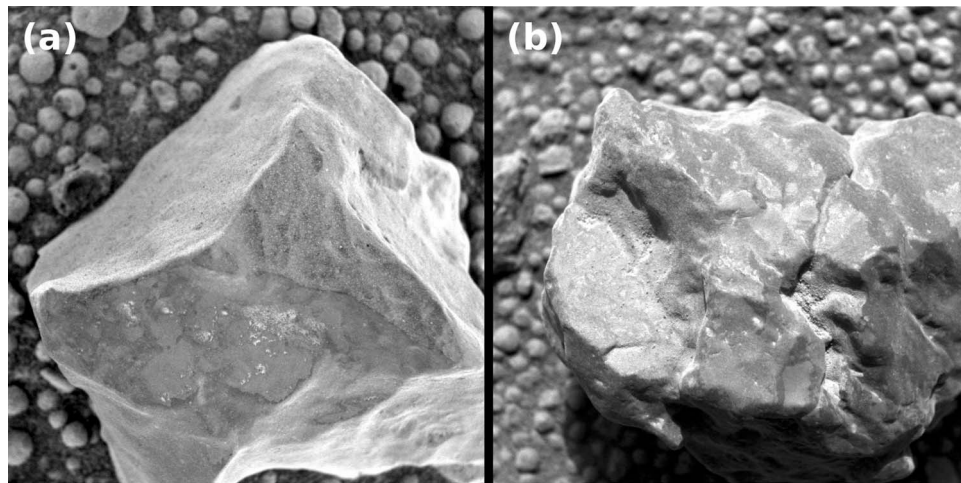


**Figure 12.** (a) MI mosaic obtained on JosephMcCoy. (b) Merge of six MI images of Perseverance acquired on sol 554. Area shown is  $\sim 3$  cm square. Both images show darker and brighter areas.

composition, as discussed in more detail by *Schröder et al.* [2008, 2009]. Compared to other meteorites, mesosiderites are uncommon, at least on Earth where they make up  $<1\%$  of observed falls. This supports the idea that the Barberton group cobbles have a common source.

[29] The similarity in composition of Barberton group cobbles raises the possibility that they are derived from a single impactor that dispersed fragments over a 7 km area. Their compositional relations make it unlikely that they were delivered to the Martian surface in several impact events [*Schröder et al.*, 2010].

[30] A delivery as secondary impact ejecta to its current location (option 2) is very plausible for the boulder Bounce Rock, which is of Martian origin (similar to SNC meteorites) and clearly not related to the site or other cobbles (J. Zipfel et al., submitted manuscript, 2010). A similar scenario appears likely for Marquette Island [*Mittlefehldt et al.*, 2010], although studies of that rock are still preliminary. Russett and Lion Stone are interpreted to be derived from local outcrop and distinctly different from any other cobbles (option 3).

[31] The origin of the Arkansas group cobbles is more difficult to determine. Most meteorite types contain metal and/or troilite, and typically have enrichments in Ni over planetary crustal materials. The compositions of Arkansas cobbles show strong similarities to rocks and especially soils at Meridiani Planum (Figures 5, 6, and 15). Therefore, we can confidently eliminate a meteoritic origin for this group. The compositional similarities of Arkansas group cobbles to locally derived materials also suggests that they are not ejecta from an area on Mars with distinctly different geology (origin 2). Their compositions do not match those of outcrop interiors (Figures 5, 6, and 15), eliminating origin 3.

[32] Material eroded from the outcrop (origin 4) includes rinds, fracture fillings and fins (probable erosional remnants of some type of fracture filling). One such target, a protruding fin of rock (“Dorsal\_Fin”), was measured in Victoria crater and was found to be similar to outcrop material, but with a substantially higher hematite content ( $\sim 50\%$  Mössbauer subspectral area), a clear difference from any of the Arkansas group cobbles. Material eroded from outcrop would be

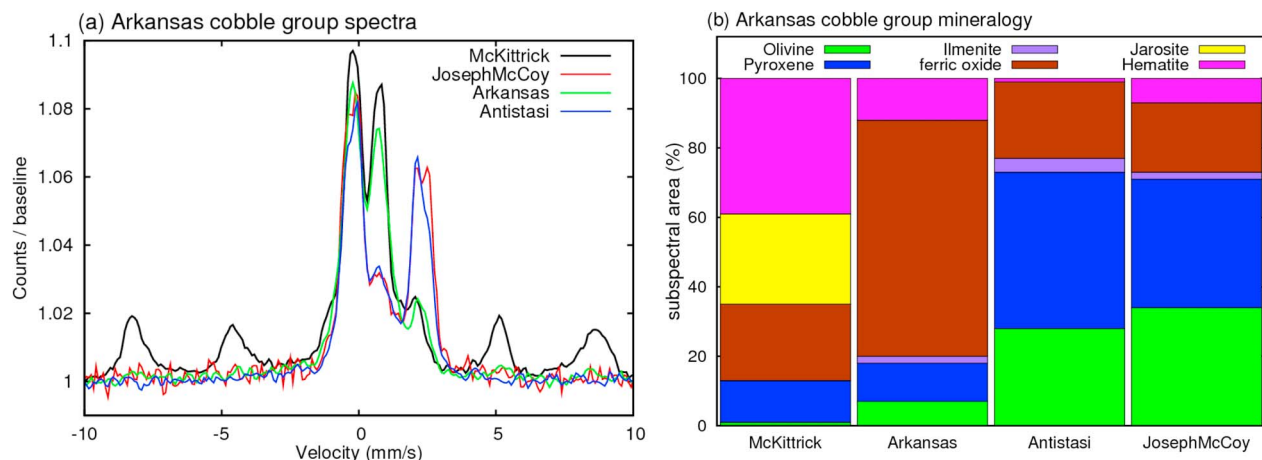


**Figure 13.** (a) Arkansas group cobbles share Mössbauer spectral features with typical outcrop. (b) Fe-bearing mineralogy determined from Mossbauer parameters. Compared to other cobble groups, a greater diversity in mineral proportions is observed among this group.

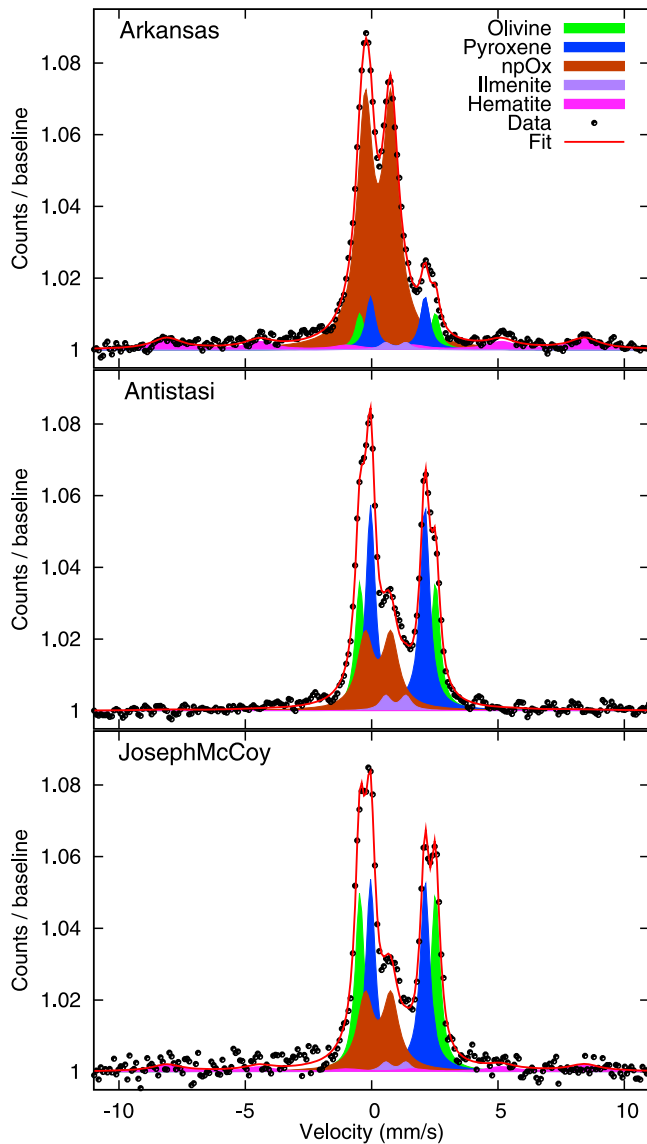


**Figure 14.** Arkansas group Mössbauer spectra with iron-bearing components derived from a simultaneous fit of all spectra.

expected to accumulate preferentially in association with outcrop exposures, which is not consistent with the observed clustering close to craters. Also, all rinds and fracture fills

that were observed in situ have a distinctive planar geometry, inconsistent with the shapes of Arkansas group cobbles. Similarly, remnants of a resistant layer that once lay above the presently exposed outcrop (origin 5) would be expected to be more evenly and commonly distributed across the plains.

[33] Remnants of a deeper layer brought to the surface by an impact (origin 6) would be expected to be more abundant across the plains. They should also be concentrated near craters large enough to excavate such a layer. This fits with the observed cobble clusters close to impact craters. However, we would expect to observe this layer deep in the crater’s stratigraphy. We have not observed a layer with different chemical, mineralogical or spectral properties than the outcrop at any location along the 20 km rover traverse or at any impact crater investigated by Opportunity, including the two largest investigated craters Victoria and Endurance. This is perhaps not surprising; because even Victoria crater would have excavated only to a depth of ~200 m. The layered sulfate-rich sediments in Meridiani Planum are substantially thicker than that [Arvidson *et al.*, 2003]. If the Arkansas group cobbles are ejecta from a deeper layer, the crater from which they were excavated must be at least tens of km from where Opportunity has traversed.

[34] With their clast-in-matrix textures (Figure 12), Arkansas group cobbles appear consistent with being impact-derived breccias and/or melts. If the clast-in-matrix texture is a correct interpretation, then we can also say that there is little differential weathering between clasts and matrix, suggesting similar hardness. Unlike outcrop rocks, spherules are not observed in the Arkansas group cobbles. Compositionally, we observe that on all elemental plots (Figures 5, 6, and 15), these cobbles appear to be compositionally similar to soils or mixtures of soils and outcrop. It is unlikely that this observation only reflects overlap of the APXS field of view with the underlying soil, since at least some cobbles are large enough to fill the instrument FOV completely. MI images indicate that their surfaces are not contaminated by dust or soil. Thus, the soil-like composition of the Arkansas cobbles is that of the cobbles, not “contaminants” in the APXS FOV.

[35] Arkansas group cobbles have Ni contents comparable to soil and outcrop (Figure 5). However, the two Arkansas group cobbles with the highest Ni content, Antistasi and JosephMcCoy (Table 2), are distinct in composition from soils with similar Ni contents. The latter are all soils rich in

**Table 4.** Mössbauer Parameters and Subspectral Areas for Arkansas Group Cobbles<sup>a</sup>

Cobble	Olivine			Pyroxene			npOx <sup>b</sup>			Ilmenite <sup>c</sup>			Hematite <sup>c</sup>			
	$\delta^d$ (mm/s)	$\Delta E_Q$ (mm/s)	A (%)	$\delta$ (mm/s)	$\Delta E_Q$ (mm/s)	A (%)	$\delta$ (mm/s)	$\Delta E_Q$ (mm/s)	A (%)	$\delta$ (mm/s)	$\Delta E_Q$ (mm/s)	A (%)	$\delta$ (mm/s)	$\Delta E_Q$ (mm/s)	$B_{hf}$ (T)	A (%)
Arkansas	1.14	3.00	7	1.15	2.23	11	0.36	1.03	72	1.07	0.81	2	0.37	-0.17 <sup>e</sup>	52.0	8
Antistasi	1.14	2.99	26	1.15	2.14	48	0.37	1.10 <sup>f</sup>	23	1.08	0.80	2	-	-	-	0
JosephMcCoy	1.14	2.96	39	1.15	2.12 <sup>e</sup>	34	0.38 <sup>e</sup>	1.03	20	1.07	0.81	2	0.37	-0.18 <sup>e</sup>	51.9	5

<sup>a</sup>Uncertainties for parameters are  $\pm 0.02$  mm/s ( $1\sigma$  deviation) for  $\delta$  and  $\Delta E_Q$  and  $\pm 0.8T$  for  $B_{hf}$  unless indicated otherwise. Uncertainties for subspectral areas are  $\pm 2\%$  (absolute).

<sup>b</sup>Abbreviation npOx: nanophase ferric oxide.

<sup>c</sup>Mössbauer hyperfine parameters for ilmenite and the center shift for hematite were held constant during the fits.

<sup>d</sup>The Mössbauer center shift  $\delta$  is given relative to  $\alpha$ -Iron.

<sup>e</sup>Uncertainty  $\pm 0.05$  mm/s.

<sup>f</sup>Uncertainty  $\pm 0.07$  mm/s.

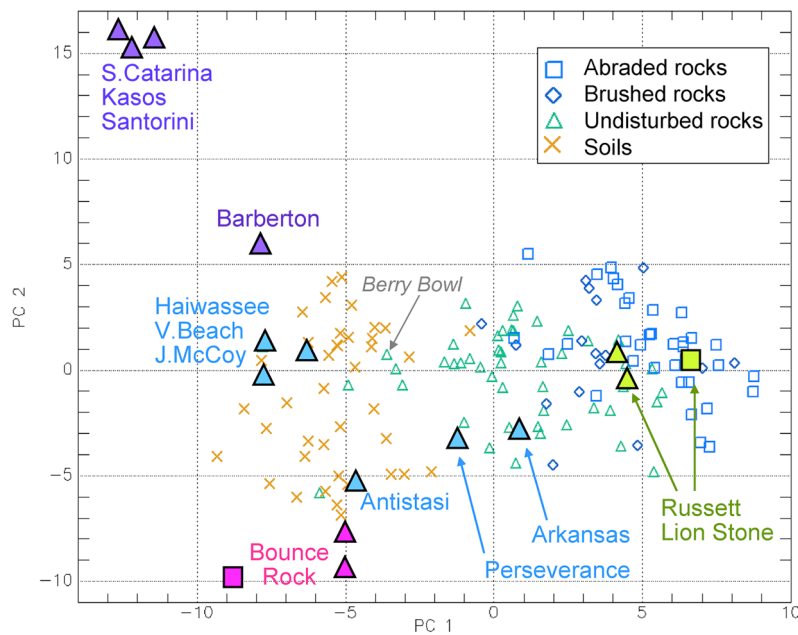


**Figure 15.** Scatterplot of the data points in the plane of the first two principal axes of the PCA performed for chemical compositions of Meridiani samples. Cobbles (violet for Barberton group; light blue for Arkansas group; light green for outcrop fragments) and Bounce Rock (magenta) are indicated with larger symbols and compared to soils (orange crosses), abraded outcrop rocks (blue squares), brushed outcrop rocks (blue diamonds), and undisturbed outcrop rocks (green triangles). The spherule-rich target “Berry Bowl” is also labeled as a reference point. For cobbles, filled triangles refer to undisturbed and filled squares refer to abraded samples.

hematitic spherules, and have much higher Fe contents than Antistasi or JosephMcCoy.

[36] The amounts of Ni in basaltic soils and Meridiani outcrop rocks were found to be consistent with a contribution of 1% to 3% chondritic input [Yen *et al.*, 2006]. An additional meteoritic component in Arkansas group cobbles from an impactor would lead to higher Ni contents (cf. Barberton group cobbles). Thus, most Arkansas group cobbles were formed from soil and/or outcrop with very little meteoritic component added during the impact that formed them. Antistasi and JosephMcCoy are possible exceptions; their higher Ni contents would allow for the addition of meteoritic material during impact melting.

[37] Most Arkansas group cobbles have Cl and S contents comparable to soil, with higher values for the Arkansas cobble. Note that SNC meteorites have considerably lower concentrations of Cl and S (Figure 6). Arkansas also has Mössbauer spectra with similarities to those of outcrop (Figure 13), and together with the high S and Cl in Arkansas, this suggests that this cobble was formed from a mixture of soil and outcrop. These results suggest that Arkansas group cobbles may represent mixtures of Meridiani outcrop and soil, consistent with impact melt, which is derived dominantly from the target material rather than the impactor [e.g., French, 1998]. Several authors have speculated about the presence of impact melt [e.g., Jolliff *et al.*, 2006; Weitz *et al.*, 2006], which would be a possible explanation for the lustrous appearance of some cobble surfaces, and also the clasts observed, which exceed the grain sizes observed in soil. Finally, because the cobbles are generally very similar to soil in composition, soil must be the major component of the

cobbles. Melting during impact would be required to produce a coherent rock from loose soil.

[38] Different cobble groups may or may not be related to each other and to observed craters. It is noteworthy that the three Arkansas group cobbles Tilos, Kos and Rhodes were found in close association with the Barberton group cobble Kasos. The physical proximity of cobble specimens belonging to different groups at this site suggests that there may indeed be a relationship between Barberton group and Arkansas group cobbles; for example, they could represent impactor fragments and impact melt breccias from the same impact.

[39] Cobbles from both groups may represent a lag of impact derived material (via fragments and impact melt breccias) that has accumulated through time [e.g., Golombek *et al.*, 2006], owing to the fact that they are harder than the Meridiani outcrop rocks.

#### 4. Conclusions

[40] Cobbles were encountered along Opportunity’s entire ~20 km traverse. On the basis of APXS elemental chemistry and Mössbauer iron mineralogy, three different groups of cobbles are distinguished. The first group comprises bright cobbles, which are texturally similar to, and chemically and mineralogically indistinguishable from outcrop and thus identified as outcrop fragments. All other cobbles appear dark in true color and false color Pancam images.

[41] The Barberton group cobbles have an ultramafic composition. Their unusually high Ni content and the presence of the Fe-bearing minerals troilite and kamacite

implicate a meteoritic origin, and their overall chemistry and mineralogy are consistent with a mesosiderite silicate clast composition.

[42] The Arkansas group cobbles appear to be related to Meridiani outcrop, with an additional basaltic – or basaltic soil – component. These cobbles have textures consistent with brecciation, pointing to an impact-related origin during which local bedrock and basaltic material from local soil were mixed (e.g., impact melt and/or breccia). The presence of many craters, some of them comparably young, is evidence for multiple impact events involved in the formation process of cobbles. Apparently, these impacts invoke the same processes forming cobbles of similar composition as a result, independent of the composition of the impactor.

[43] **Acknowledgments.** I.F. and G.K. acknowledge support from the German Space Agency (DLR; contracts 50 QM 9902 (Mössbauer MIMOS II) and 50 QM 0005 (APXS)) and the University of Mainz. We acknowledge the unwavering support of JPL engineering and MER operations staff and the MER Athena Science Team. D. G. Agresti is acknowledged for providing the MERFit program. We thank two external referees for thoughtful reviews of the manuscript.

## References

- Agresti, D. G., and P. A. Gerakines (2009), Simultaneous fitting of Mars Mössbauer data, *Hyperfine Interact.*, **188**, 113–120, doi:10.1007/s10751-008-9896-1.
- Arvidson, R. E., F. P. Seelos, K. S. Deal, W. C. Koeppen, N. O. Snider, J. M. Kieniewicz, B. M. Hynek, M. T. Mellon, and J. B. Garvin (2003), Mantled and exhumed terrains in Terra Meridiani, Mars, *J. Geophys. Res.*, **108**(E12), 8073, doi:10.1029/2002JE001982.
- Ashley, J. W., S. W. Ruff, A. T. Knudson, and P. R. Christensen (2009), Mini-TES measurements of Santa Catarina-type, stony-iron meteorite candidates by the Opportunity rover, *Lunar Planet. Sci.*, **XL**, Abstract 2468.
- Bell, J. F., et al. (2003), Mars Exploration Rover Athena Panoramic Camera (Pancam) investigation, *J. Geophys. Res.*, **108**(E12), 8063, doi:10.1029/2003JE002070.
- Bogard, D. D., and P. Johnson (1983), Martian gases in an Antarctic meteorite?, *Science*, **221**, 651–654, doi:10.1126/science.221.4611.651.
- Brückner, J., G. Dreibus, R. Gellert, S. W. Squyres, H. Wänke, A. Yen, and J. Zipfel (2008), Mars Exploration Rovers - Chemical composition by APXS, in *The Martian Surface: Composition, Mineralogy, and Physical Properties*, edited by J. Bell, pp. 58–102, Cambridge Univ. Press, New York, doi:10.1017/CBO9780511536076.005.
- Christensen, P. R., et al. (2003), Miniature Thermal Emission Spectrometer for the Mars Exploration Rovers, *J. Geophys. Res.*, **108**(E12), 8064, doi:10.1029/2003JE002117.
- Connolly, H. C., et al. (2006), The Meteoritical Bulletin, No. 90, 2006 September, *Meteorit. Planet. Sci.*, **41**(9), 1383–1418, doi:10.1111/j.1945-5100.2006.tb00529.x.
- Dreibus, G., B. Huisl, B. Spettel, and R. Haubold (2003), Comparison of the chemistry of Y-000593 and Y-000749 with other nakhlites, *Lunar Planet. Sci.*, [CD-ROM] **XXXIV**, Abstract 1586.
- Farrand, W. H., et al. (2007), Visible and near-infrared multispectral analysis of rocks at Meridiani Planum, Mars, by the Mars Exploration Rover Opportunity, *J. Geophys. Res.*, **112**, E06S02, doi:10.1029/2006JE002773.
- Farrand, W. H., J. F. Bell III, J. R. Johnson, R. E. Arvidson, L. S. Crumpler, J. A. Hurowitz, and C. Schröder (2008), Rock spectral classes observed by the Spirit Rover's Pancam on the Gusev Crater Plains and in the Columbia Hills, *J. Geophys. Res.*, **113**, E12S38, doi:10.1029/2008JE003237.
- French, B. M. (1998), *Traces of Catastrophe: A Handbook of Shock-Metamorphic Effects in Terrestrial Meteorite Impact Structures*, Lunar Planet. Inst., Houston, Tex.
- Golombek, M. P., et al. (2006), Erosion rates at the Mars Exploration Rover landing sites and long-term climate change on Mars, *J. Geophys. Res.*, **111**, E12S10, doi:10.1029/2006JE002754.
- Golombek, M., K. Robinson, A. McEwen, N. Bridges, B. Ivanov, L. Tornabene, and R. Sullivan (2010), Constraints on ripple migration at Meridiani Planum from observations of fresh craters by Opportunity and HiRISE, *Lunar Planet. Sci.*, **XL1**, Abstract 2373.
- Gorevan, S. P., et al. (2003), Rock Abrasion Tool: Mars exploration Rover mission, *J. Geophys. Res.*, **108**(E12), 8068, doi:10.1029/2003JE002061.
- Herkenhoff, K. E., et al. (2003), Athena Microscopic Imager investigation, *J. Geophys. Res.*, **108**(E12), 8065, doi:10.1029/2003JE002076.
- Herkenhoff, K. E., et al. (2008), Surface processes recorded by rocks and soils on Meridiani Planum, Mars: Microscopic Imager observations during Opportunity's first three extended missions, *J. Geophys. Res.*, **113**, E12S32, doi:10.1029/2008JE003100.
- Jolliff, B. L., W. H. Farrand, J. R. Johnson, C. Schröder, and C. M. Weitz (2006), Origin of rocks and cobbles on the Meridiani Plains as seen by Opportunity, *Lunar Planet. Sci.*, **XXXVII**, Abstract 2401.
- Klingelhöfer, G., et al. (2003), Athena MIMOS II Mössbauer spectrometer investigation, *J. Geophys. Res.*, **108**(E12), 8067, doi:10.1029/2003JE002138.
- Krumbein, W. C., and L. L. Sloss (1963), *Stratigraphy and Sedimentation*, 2nd ed., Freeman, San Francisco, Calif.
- McSween, H. Y., Jr., E. M. Stolper, L. A. Taylor, R. A. Muntean, G. D. O'Kelley, J. S. Eldridge, S. Biswas, H. T. Ngo, and M. E. Lipschutz (1979), Petrogenetic relationship between Allan Hills 77005 and other achondrites, *Earth Planet. Sci. Lett.*, **45**, 275–284, doi:10.1016/0012-821X(79)90129-8.
- Mittlefehldt, D. W., et al. (2010), Marquette Island: A distinct mafic lithology discovered by Opportunity, *Lunar Planet. Sci.*, [CD-ROM] **XL1**, Abstract 2109.
- Morris, R. V., et al. (2006a), Mössbauer mineralogy of rock, soil, and dust at Gusev crater, Mars: Spirit's journey through weakly altered olivine basalt on the plains and pervasively altered basalt in the Columbia Hills, *J. Geophys. Res.*, **111**, E02S13, doi:10.1029/2005JE002584.
- Morris, R. V., et al. (2006b), Mössbauer mineralogy of rock, soil, and dust at Meridiani Planum, Mars: Opportunity's journey across sulfate-rich outcrop, basaltic sand and dust, and hematite lag deposits, *J. Geophys. Res.*, **111**, E12S15, doi:10.1029/2006JE002791.
- Morris, R. V., et al. (2008), Iron mineralogy and aqueous alteration from Husband Hill through Home Plate at Gusev Crater, Mars: Results from the Mössbauer instrument on the Spirit Mars Exploration Rover, *J. Geophys. Res.*, **113**, E12S42, doi:10.1029/2008JE003201.
- Nuding, D. L., and B. A. Cohen (2009), Characterization of rock types at Meridiani Planum, Mars using MER 13-filter Pancam spectra, *Lunar Planet. Sci.*, **XL**, Abstract 2023.
- Nyquist, L. E., D. D. Bogard, J. L. Wooden, H. Wiesmann, C.-Y. Shih, B. M. Bansal, and G. A. McKay (1979), Early differentiation, late magmatism, and recent bombardment on the shergottite parent planet, *Meteoritics*, **14**, 502.
- Rieder, R., R. Gellert, J. Brückner, G. Klingelhöfer, G. Dreibus, A. Yen, and S. W. Squyres (2003), The new Athena alpha particle X-ray spectrometer for the Mars Exploration Rovers, *J. Geophys. Res.*, **108**(E12), 8066, doi:10.1029/2003JE002150.
- Schröder, C., et al. (2008), Meteorites on Mars observed with the Mars Exploration Rovers, *J. Geophys. Res.*, **113**, E06S22, doi:10.1029/2007JE002990.
- Schröder, C., et al. (2009), Santorini, another meteorite on Mars and third of a kind, *Lunar Planet. Sci.*, **XL**, Abstract 1665.
- Schröder, C., et al. (2010), Properties and distribution of paired stony meteorite candidate rocks at Meridiani Planum, Mars, *J. Geophys. Res.*, doi:10.1029/2010JE003616, in press.
- Squyres, S. W., et al. (2003), Athena Mars rover science investigation, *J. Geophys. Res.*, **108**(E12), 8062, doi:10.1029/2003JE002121.
- Squyres, S. W., et al. (2006), Overview of the Opportunity Mars Exploration Rover mission to Meridiani Planum: Eagle crater to Purgatory ripple, *J. Geophys. Res.*, **111**, E12S12, doi:10.1029/2006JE002771.
- Squyres, S. W., et al. (2009), Exploration of Victoria Crater by the Mars Rover Opportunity, *Science*, **324**(5930), 1058–1061, doi:10.1126/science.1170355.
- Stevens, J. G., A. M. Khasanov, J. W. Miller, H. Pollak, and Z. Li (2002), *Mössbauer Mineral Handbook*, Mössbauer Effect Data Cent., Asheville, N. C.
- Tréguier, E., C. d'Uston, P. C. Pinet, G. Berger, M. J. Toplis, T. J. McCoy, R. Gellert, and J. Brückner (2008), Overview of Mars surface geochemical diversity through Alpha Particle X-Ray Spectrometer data multidimensional analysis: First attempt at modeling rock alteration, *J. Geophys. Res.*, **113**, E12S34, doi:10.1029/2007JE003010.
- Treiman, A. H., J. D. Gleason, and D. D. Bogard (2000), The SNC meteorites are from Mars, *Planet. Space Sci.*, **48**, 1213–1230, doi:10.1016/S0032-0633(00)00105-7.
- Walker, D., E. M. Stolper, and J. F. Hays (1979) Basaltic volcanism: The importance of Planet size, *Proc. Lunar Planet. Sci. Conf.*, **10th**, 1995–2015.
- Wasson, J. T., and G. W. Wetherill (1979), Dynamical chemical and isotopic evidence regarding the formation locations of asteroids and meteorites, in *Asteroids*, edited by T. Gehrels, pp. 926–974, Univ. of Ariz. Press, Tucson.

- Weitz, C. M., R. C. Anderson, J. F. Bell, W. H. Farrand, K. E. Herkenhoff, J. R. Johnson, B. L. Jolliff, R. V. Morris, S. W. Squyres, and R. J. Sullivan (2006), Soil grain analyses at Meridiani Planum, Mars, *J. Geophys. Res.*, *111*, E12S04, doi:10.1029/2005JE002541.
- Weitz, C. M., et al. (2010), Visible and near-infrared multispectral analysis of geochemically measured rock fragments at the Opportunity landing site in Meridiani Planum, *J. Geophys. Res.*, doi:10.1029/2010JE003660, in press.
- Yen, A. S., et al. (2006), Nickel on Mars: Constraints on meteoritic material at the surface, *J. Geophys. Res.*, *111*, E12S11, doi:10.1029/2006JE002797.
- 
- J. Ashley, Mars Space Flight Facility, School of Earth and Space Exploration, Arizona State University, PO Box 876305, Tempe, AZ 85287, USA.
- J. Brückner, Max-Planck-Institut für Chemie, Johann-Joachim-Becher-Weg 27, PO Box 3060, D-55020 Mainz, Germany.
- B. A. Cohen, Lunar Quest Program, NASA Marshall Space Flight Center, VP 62, 320 Sparkman Dr., Huntsville, AL 35812, USA.
- P. A. de Souza, Tasmanian ICT Centre, CSIRO, GPO Box 1538, Hobart, Tas 7001, Australia.
- W. Farrand, Space Science Institute, 4750 Walnut St., Ste. 205, Boulder, CO 80301, USA.
- I. Fleischer and G. Klingelhöfer, Institut für Anorganische Chemie und Analytische Chemie, Johannes Gutenberg-Universität, Staudinger Weg 9, D-55128 Mainz, Germany. (fleischi@uni-mainz.de)
- R. Gellert, Department of Physics, University of Guelph, Guelph, ON N1G 2W1, Canada.
- M. Golombek, Jet Propulsion Laboratory, California Institute of Technology, Mail Stop 183-501, 4800 Oak Grove Dr., Pasadena, CA 91109, USA.
- K. Herkenhoff and J. R. Johnson, Astrogeology Science Center, U.S. Geological Survey, 2255 N. Gemini Dr., Flagstaff, AZ 86001, USA.
- B. Jolliff, Department of Earth and Planetary Sciences, Washington University in St. Louis, 1 Brookings Dr., St. Louis, MO 63130, USA.
- D. Mittlefehldt and R. V. Morris, NASA Johnson Space Center, ARES Mail Code KR, 2101 NASA Parkway, Houston, TX 77058, USA.
- C. Schröder, Center for Applied Geoscience, Eberhard Karls University of Tübingen, Sigwartstr. 10, D-72076 Tübingen, Germany.
- S. W. Squyres, Department of Astronomy, Cornell University, 428 Space Sciences Bldg., Ithaca, NY 14853, USA.
- E. Tréguier, European Space Astronomy Centre, PO Box 78, E-28691 Villanueva de la Cañada, Madrid, Spain.
- C. Weitz, Planetary Science Institute, 1700 East Fort Lowell, Ste. 106, Tucson, AZ 85719, USA.